

# Analytical Methods

Accepted Manuscript



This is an *Accepted Manuscript*, which has been through the Royal Society of Chemistry peer review process and has been accepted for publication.

*Accepted Manuscripts* are published online shortly after acceptance, before technical editing, formatting and proof reading. Using this free service, authors can make their results available to the community, in citable form, before we publish the edited article. We will replace this *Accepted Manuscript* with the edited and formatted *Advance Article* as soon as it is available.

You can find more information about *Accepted Manuscripts* in the [Information for Authors](#).

Please note that technical editing may introduce minor changes to the text and/or graphics, which may alter content. The journal's standard [Terms & Conditions](#) and the [Ethical guidelines](#) still apply. In no event shall the Royal Society of Chemistry be held responsible for any errors or omissions in this *Accepted Manuscript* or any consequences arising from the use of any information it contains.

1  
2  
3  
4 1 **Magnetic solid-phase extraction of proteins based on hydroxy**  
5  
6 2 **functional ionic liquids modified magnetic nanoparticles**  
7  
8  
9 3

10 4 Jing Chen, Yuzhi Wang\*, Xueqin Ding, Yanhua Huang ,Kaijia Xu

11 5 State Key Laboratory of Chemo/Biosensing and Chemometrics, College of

12 6 Chemistry and Chemical Engineering, Hunan University, Changsha, 410082, P.R.

13 7  
14  
15  
16  
17 8  
18 9 China  
19  
20  
21  
22  
23

24 9 **Corresponding author: Professor Yuzhi Wang**

25 10 State Key Laboratory of Chemo/Biosensing and Chemometrics

26 11 College of Chemistry and Chemical Engineering

27 12 Hunan University

28 13 Changsha 410082

29 14 P. R. China

30 15 Phone: +86-731-88821903

31 16 Fax: +86-731-88821848

32 17 E-mail: [wyzss@hnu.edu.cn](mailto:wyzss@hnu.edu.cn)  
33  
34  
35  
36  
37  
38  
39  
40  
41  
42  
43  
44  
45  
46  
47  
48  
49  
50  
51  
52  
53  
54  
55  
56  
57  
58  
59  
60

1  
2  
3  
4 24 **Abstract**  
5

6 Hydroxy functional ionic liquids has been first designed and modified on the  
7  
8 surface of silica-coated magnetic Fe<sub>3</sub>O<sub>4</sub> nanoparticles (MNPs) for the investigation of  
9  
10 the extraction performance of proteins by magnetic solid-phase extraction (MSPE)  
11  
12 and characterized by fourier transform infrared spectroscopy (FTIR),electron  
13  
14 microscopy (TEM), vibrating sample magnetometer(VSM), X-ray diffraction (XRD)  
15  
16 and thermo gravimetric analysis (TGA). BSA was chosen as a model protein to  
17  
18 investigate the effect of extraction parameters. Based on the single-factor experiment,  
19  
20 an initial serial investigative test was used to identify the optimal conditions of the  
21  
22 extraction and the extraction efficiency could reach up to 86.92%. The RSD of  
23  
24 extraction efficiencies in precision experiment, repeatability experiment and stability  
25  
26 experiment were 1.17% (n=3), 3.79% (n=3) and 4.82% (n=3), respectively. Compared  
27  
28 with other four types of ionic liquids, hydroxy functional ionic liquids modified  
29  
30 magnetic nanoparticles has the highest extraction rate. Desorption of proteins was up  
31  
32 to 94.91% when the concentrations of NaCl greater than 1.1 mol L<sup>-1</sup>. Nearly 95% of  
33  
34 MNPs could be recovered from each run and extraction rate decreased significantly  
35  
36 after five runs.  
37  
38  
39  
40  
41  
42  
43  
44  
45  
46  
47  
48  
49  
50  
51  
52  
53  
54  
55  
56  
57  
58  
59  
60

42 **Keywords:** Magnetic nanoparticle, Hydroxy functional ionic liquids, Solid-phase  
43 extraction, Protein

## 1. Introduction

Proteins play a critical role in the basis of life like antibodies in animal immune response, metabolism, gene expression, signal transduction, nutrients, and even as cellular extracellular structures, etc [1]. However, proteins always exist within complex mixtures and poor stability in the conditions of acids, alkali or heating. Therefore, it is necessary to prepare the technology of protein purification and identification.

The classic methods for protein purification include ammonium sulfate precipitation, salting out, electrophoresis [2]. Current techniques for the pre-concentration of protein include ionic or affinity chromatography [3], ionic liquid aqueous two-phase system [4,5], solid phase extraction (SPE) [6], solid-phase microextraction (SPME), pressurized liquid extraction and supercritical fluid extraction.

In recent years, nanoparticles are being paid more and more attention for separation purposes. Nanoparticles have large specific surface areas, thus a large fraction of active sites are available for appropriate chemical interaction [7]. In the numerous nanoparticles, because of the magnetic nanoparticles can be isolated by a magnetic plate from the reaction medium, they have been widely researched. But, the naked magnetic nanoparticles have a low adsorption on account of large solute molecules such as proteins which cannot be specific adsorption. So many organic functional monomers or polymers have been modified on the magnetic nanoparticles

1  
2  
3  
4 68 such as polyacrylic acid [8], tetrabenzyl [9], polyacrylamide [10], diphenyl [11],  
5  
6 69 phosphatidylcholine [12] and so on.  
7

8  
9 70 Ionic liquids (ILs) are a class of liquids which were first reported by Walden in  
10  
11 71 1941 [13]. ILs have many fascinating properties including wide liquid ranges, low  
12  
13 72 volatilities (negligible vapor pressure), good thermal stabilities, electrolytic  
14  
15 73 conductivity, wide range of viscosities, adjustable miscibility, reusability,  
16  
17 74 nonflammability and so on [14]. The greatest feature of ionic liquids is designing. By  
18  
19 75 adjusting the combination or introducing an appropriate functional groups, the  
20  
21 76 specific ionic liquids can be obtained. But the ionic liquids which directly used for  
22  
23 77 protein extraction, can not only cause changes in protein conformation, but also loss  
24  
25 78 activity and be difficult to recycle and reuse.  
26  
27  
28  
29  
30

31 79 To solve this problem, ionic liquid-modified on the surface of the magnetic  
32  
33 80 nanoparticles (ILs-MNPs) which consist of bulky organic cations combining with  
34  
35 81 inorganic or organic anions, has recently been developed as a new sorbent material.  
36  
37 82 Because the magnetic  $\text{Fe}_3\text{O}_4$  nanoparticles easy to be oxidized and large aggregated,  
38  
39 83 before the ionic liquid modified on the surface of magnetic nanoparticles, coated with  
40  
41 84 a layer of silicon is very necessary. The silica-shell coated on the surface of  $\text{Fe}_3\text{O}_4$   
42  
43 85 nanoparticles can prevent the oxidation of  $\text{Fe}_3\text{O}_4$  and the surface silanol groups could  
44  
45 86 offer many possibilities for further surface modification, such as the introduction of  
46  
47 87 hydroxyl, carboxyl, amino groups. In addition it also could improve the corrosion  
48  
49 88 resistance, chemically stability and effectively reduce the aggregation of  $\text{Fe}_3\text{O}_4$   
50  
51 89 nanoparticles in the liquid.  
52  
53  
54  
55  
56  
57  
58  
59  
60

1  
2  
3  
4 90 ILs-MNPs have been applied in magnetic solid-phase extraction (MSPE) of  
5  
6 91 various compounds such as flavonoids [15,16], ergosterol [17], lipase [18], Dye [7,13],  
7  
8  
9 92 DNA [19],metals [20], phthalate esters [21-24], sulfonylurea herbicides [25] and  
10  
11 93 enzymes [26-29]. Some others had studied the applications of ILs-MNPs as recyclable  
12  
13  
14 94 catalyst [30-34]. An alluring prospect is that the protein adsorbed on magnetic  
15  
16 95 nanoparticles modified by ionic liquids can be separated by applying magnetic field,  
17  
18  
19 96 which conducive to recycle and reuse for multiple times.

20  
21  
22 97 To the best of our knowledge, adsorption of proteins on magnetic silica  
23  
24 98 nanoparticles modified by hydroxy functional ionic liquids has not been reported.  
25  
26  
27 99 Herein, five environmental-friendly hydrophilic ionic liquids (ILs) were synthesized  
28  
29  
30 100 and modified on the surface of silica-coated magnetic Fe<sub>3</sub>O<sub>4</sub> nanoparticles (SiO<sub>2</sub>@  
31  
32 101 Fe<sub>3</sub>O<sub>4</sub>) for the investigation of the extraction performance of proteins by magnetic  
33  
34  
35 102 solid-phase extraction (as shown in scheme 1). [Simam][Cl]-MNPs were chosen as  
36  
37  
38 103 a model. The concentrations of proteins in solution were determined by measuring the  
39  
40 104 absorbance at 278 nm for bovine serum albumin (BSA) and ovalbumin (OVA), and at  
41  
42 105 404 nm for bovine hemoglobin (BHb). BSA was chosen as a model protein to  
43  
44  
45 106 investigate the effect of system parameters. Adsorption isotherms, kinetic of  
46  
47  
48 107 adsorption, recycling and reusing of the sorbent were characterized as well.

## 108 **2. Experimental**

### 109 **2.1 Instrumentation**

110 The mainly used instruments included: DZF-6051 vacuum drying oven (Shanghai,  
111 China), D5000 X-ray Diffraction (Siemens, Japan), Thermostats cultivating shaker

1  
2  
3  
4 112 (Shanghai, China), UV-2450 UV-Vis Spectrophotometer (SHIMADZU, Japan),  
5  
6 113 VarianInova-400 NMR spectrometer (Varian, USA), FT-IR spectrometer  
7  
8  
9 114 (PerkinElmer, USA), JEM-1230 transmission electron microscope (JEOL, Japan),  
10  
11 115 STA 409 thermal gravimetric analyzer (Netzsch, Germany) and EV 11 Vibrating  
12  
13  
14 116 Sample Magnetometer (MicroSense, USA).

## 15 16 117 **2.2 Chemicals and reagents**

17  
18  
19 118 Iron (II) sulfate heptahydrate ( $\text{FeSO}_4 \cdot 7\text{H}_2\text{O}$ ), iron (III) chloride hexahydrate  
20  
21 119 ( $\text{FeCl}_3 \cdot 6\text{H}_2\text{O}$ ), ammonia solution (27%, w/v), hydrazine hydrate, and 2-propanol were  
22  
23  
24 120 purchased from Fuchen (Tianjin, China). Tetraethyl orthosilicate (TEOS), toluene,  
25  
26 121 N-Methylimidazole, were purchased from Aladdin chemistry Co. Ltd. (Shanghai,  
27  
28  
29 122 China). N, N-dimethylethanolamine (DMEA) and pyrrole were purchased from  
30  
31 123 Tianjin Kermel Fine Chemical Research Institute. N-Ethylmorpholine, 1,1,3,3-tetrame  
32  
33  
34 124 thylguanidine were obtained from Energy Chemical Company (Shanghai, China).  
35  
36 125 BSA, ethyl acetate, and other reagents were supplied by Sinopharm Chemical  
37  
38  
39 126 Reagent Co., Ltd. (Shanghai, China). All the chemicals from the commercial sources  
40  
41  
42 127 were generally of analytical grade without any further purification.

## 43 44 128 **2.3 Grafting of ILs at the surface of magnetic nanoparticles (IL-SiO<sub>2</sub>@ Fe<sub>3</sub>O<sub>4</sub>)**

45  
46 129 The nanoparticles of  $\text{Fe}_3\text{O}_4$  were synthesized by the improved coprecipitation  
47  
48  
49 130 method. In order to get the maximum yield for magnetic nanoparticles, the ideal  
50  
51 131 molar ratio of  $\text{Fe}^{2+}/\text{Fe}^{3+}$  was about 0.5 (as shown in Scheme 2: Step 1 ). So 5.41 g of  
52  
53  
54 132  $\text{FeCl}_3 \cdot 6\text{H}_2\text{O}$  was dissolved in 30 mL of water, and then 1 mL hydrazine hydrate and  
55  
56  
57 133 2.78 g  $\text{FeSO}_4 \cdot 7\text{H}_2\text{O}$  were sequentially added to the solution. After dissolved  
58  
59  
60

1  
2  
3  
4 134 thoroughly, 10 mL ammonium hydroxide (27%, w/v) was quickly added to the  
5  
6 135 solution under violently stirring, then to make sure the pH value of the solution was 9.  
7  
8  
9 136 The reaction was maintained for 30 min at room temperature. Then the mixture was  
10  
11 137 cured for 1 h at 80 °C. The magnetite precipitates were isolated by a magnetic plate  
12  
13 138 from the reaction medium and washed several times with deionized water until the  
14  
15 139 washing solution was neutral. Finally the magnetic Fe<sub>3</sub>O<sub>4</sub> nanoparticles were washed  
16  
17 140 with anhydrous ethanol for three times and dried in vacuum drying oven at 70 °C for  
18  
19 141 24 h.  
20  
21  
22  
23

24 142 The method of modified Fe<sub>3</sub>O<sub>4</sub> nanoparticles with silicon was reported in our  
25  
26 143 previous work [35]. 600 mg Fe<sub>3</sub>O<sub>4</sub> was diluted with 10 mL of water and 50 mL of  
27  
28 144 2-propanol by ultrasonic vibration for 30 min. 10 mL ammonia solution and 4 mL  
29  
30 145 TEOS were added at room temperature with stirring for 12 h in order to allow the  
31  
32 146 silica shell to grow on the surface of the nanoparticles (as shown in Scheme 2. Step:  
33  
34 147 1 ). The suspension was isolated by a magnetic plate and washed with ultra pure water  
35  
36 148 until the pH of washing solution was 7. Finally the particles were dried under vacuum  
37  
38 149 at 70 °C for 24 h.  
39  
40  
41  
42  
43

44 150 With the moderate modification of the method in the literature [25,31], five kinds  
45  
46 151 of ionic liquids consisting of chloride anions and different cations (as shown in Table  
47  
48 152 1) were synthesized: 1-methyl-3-(triethoxy) silypropyl-imidazolium  
49  
50 153 chloride([Simim][Cl]), (2-hydroxyethyl)-N,N-dimethyl-3-(triethoxy)  
51  
52 154 silypropyl-ammonium chloride([Simam][Cl]), N-ethyl-N-[3-(triethoxy)  
53  
54 155 silypropyl]-morpholinium chloride([Siemp][Cl]), N,N,N',N'-tetramethyl-3-(triethoxy)  
55  
56  
57  
58  
59  
60



1  
2  
3  
4 156 silypropyl-guanidinium chloride([Sitmg][Cl]), N-methyl-N-[3-(triethoxy)  
5  
6 157 silypropyl]-pyrrolium chloride([Simpyl][Cl]) were directly synthesized in just one step.  
7  
8  
9 158 The synthetic route of the ionic liquids was shown in Scheme 2: Step 2. As an  
10  
11 159 example, a 250 mL round-bottom flask equipped with a magnetic stirring bar and  
12  
13 160 condenser was charged with 20 mmol of 3-Chloropropyltriethoxysilane and 20 mmol  
14  
15 161 of N,N-dimethylaminoethanol. The mixture was refluxed with stirring for 8 h at  
16  
17 162 120 °C. After the reaction had cooled to room, the product was purified further by  
18  
19 163 washing three times with 100 mL of ethyl acetate, and then dried in a vacuum for  
20  
21 164 24h. The five kinds of ionic liquids structures were confirmed by FT-IR, <sup>1</sup>H NMR and  
22  
23 165 <sup>13</sup>C NMR spectra, which were shown in supplementary data Table S1 and Fig.S1,  
24  
25 166 respectively.  
26  
27  
28  
29  
30

31 167 100 mg silica-coated nanoparticles were dissolved in 100 mL toluene by  
32  
33 168 ultrasonication for 15 min. One gram IL was then added to the system and the mixture  
34  
35 169 was stirred at 120 °C for two days (as shown in Scheme 2: Step 3). After reaction, the  
36  
37 170 nanoparticles were washed with water for two times and with ethanol for three times.  
38  
39 171 Finally the particles were dried under vacuum at 70 °C for 24 h.  
40  
41  
42  
43

#### 44 172 **2.4 Magnetic Solid-phase extraction procedure**

45  
46 173 Adsorption of protein from aqueous solutions on the surfaces of biofunctional  
47  
48 174 magnetic nanoparticles was investigated batch-wise. The schematic diagram of the  
49  
50 175 extraction process was shown in Scheme 3. Different amount of the IL-MNPs were  
51  
52 176 added into the protein solutions which were shaken at 200 rpm for a predefined time  
53  
54 177 and temperature. After extraction, the solid phase which contained adsorbed protein  
55  
56  
57  
58  
59  
60

1  
2  
3  
4 178 on the surface of ILs-MNPs was magnetically separated. The amounts of protein  
5  
6 179 adsorbed on the magnetic nano-adsorbents were estimated from the concentration  
7  
8  
9 180 change of protein in solution after adsorption by UV–vis spectrometer at absorbance  
10  
11 181 at 278 nm for bovine serum albumin (BSA) and ovalbumin (OVA), and at 404 nm for  
12  
13  
14 182 bovine hemoglobin (BHb) for protein assay. The extraction efficiency (E) was  
15  
16 183 calculated by the following equation:

$$17 \quad 184 \quad E = (C_o - C_e) \times 100\% / C_o \quad (1)$$

18  
19  
20  
21 185 Where  $C_o$  is the initial protein concentrations (mg mL<sup>-1</sup>),  $C_e$  is the equilibrium  
22  
23 186 protein concentrations (mg mL<sup>-1</sup>).

24  
25  
26 187 Desorption of protein from the surface of IL-MNPs (after extracting through  
27  
28 188 optimum extraction conditions) was conducted with addition of NaCl. The desorption  
29  
30  
31 189 ratios (D) was calculated using the following equation:

$$32 \quad 33 \quad 34 \quad 35 \quad 36 \quad 37 \quad 38 \quad 39 \quad 40 \quad 41 \quad 42 \quad 43 \quad 44 \quad 45 \quad 46 \quad 47 \quad 48 \quad 49 \quad 50 \quad 51 \quad 52 \quad 53 \quad 54 \quad 55 \quad 56 \quad 57 \quad 58 \quad 59 \quad 60 \quad D = C_r / (C_o - C_e) \times 100\% \quad (2)$$

191 Where  $C_r$  is the concentration of protein in the desorption medium.

## 192 **2.5 Recycling and reusing of the ILs-MNPs**

193 The recycling and reusing of the ILs-MNPs are highly preferable for a greener  
194 process. After protein desorption by NaCl solution with different ionic strength, the  
195 magnetic nanoparticles can be isolated by simple magnetic decantation using a  
196 magnetic plate. The ILs-MNPs can be reused after washing with ethanol and drying in  
197 vacuum at 70 °C for 24 h then reused in a subsequent reaction.

## 198 **3. Results and discussion**

### 199 **3.1 Characterization of the ILs-MNPs**

1  
2  
3  
4 200 FT-IR spectroscopy was employed to certify the successful modification of  
5  
6 201 magnetic nanoparticles with ILs (as shown in Fig. 1). The strong bond around 569  
7  
8 202  $\text{cm}^{-1}$  corresponds to Fe–O vibrations of the magnetite core which can be observed in  
9  
10  
11 203 every curve. The characteristic bands around  $1101.42 \text{ cm}^{-1}$ ,  $925.27 \text{ cm}^{-1}$  and  $464.06$   
12  
13 204  $\text{cm}^{-1}$  which were assigned to the Si–O–Si asymmetric stretching vibration, Si–C  
14  
15  
16 205 stretching vibration and Si–O–Si bending vibration, respectively, can be observed  
17  
18  
19 206 after modified  $\text{Fe}_3\text{O}_4$  nanoparticles with silicon. The spectrum also displays strong  
20  
21 207 bands around  $3370$  and  $1607 \text{ cm}^{-1}$ , which were assigned to O–H stretching, N–H  
22  
23 208 stretching, and H–O–H bending modes of vibration, respectively. The distinguished  
24  
25  
26 209 feature in the FT-IR spectra of ILs bonded to silica-coated nanoparticles was the  
27  
28  
29 210 appearance of the new peak around  $2949$  and  $2882 \text{ cm}^{-1}$ , which was assigned to the  
30  
31 211 symmetric and asymmetric methylene ( $\text{CH}_2$ ) and methyl ( $\text{CH}_3$ ) vibrations. It was  
32  
33  
34 212 notable that lots of new peaks (such as  $1607.47$ ,  $1479.36 \text{ cm}^{-1}$ ) can be found after  
35  
36  
37 213 modified ionic liquids on the magnetic nanoparticles which proved that the ionic  
38  
39 214 liquids were successfully modified on the surface of  $\text{SiO}_2@\text{Fe}_3\text{O}_4$  MNPs.

40  
41 215 TGA was performed to further estimate the relative composition of core and the  
42  
43  
44 216 amount of ionic liquid deposited onto the surface of  $\text{SiO}_2@\text{Fe}_3\text{O}_4$ . Based on the  
45  
46  
47 217 thermograms provided in Fig. 2, it can be seen that there is an initial loss of weight at  
48  
49 218 temperature below  $200 \text{ }^\circ\text{C}$  for all samples. This is attributed to the removal of water  
50  
51  
52 219 and solvent residues. The bond energy of Si–O–Fe is great, and the silica coating on  
53  
54 220 the  $\text{Fe}_3\text{O}_4$  nanoparticles can withstand high temperature, so the weight loss of  
55  
56  
57 221  $\text{SiO}_2@\text{Fe}_3\text{O}_4$  MNPs is very little when the temperature exceeds  $200 \text{ }^\circ\text{C}$ . When the  
58  
59  
60

1  
2  
3  
4 222 temperature continues to rise over 300 °C, the weight loss of curves c was due to the  
5  
6 223 decomposition of ionic liquid. According to the TGA curves, the ionic liquid content  
7  
8  
9 224 of silica-coated magnetic nanoparticles was evaluated to be in excess of 35% by  
10  
11 225 weight.

12  
13  
14 226 The XRD spectra is used for determining the crystallographic identity of the  
15  
16 227 produced material, phase purity and for calculating the mean particle size based on the  
17  
18  
19 228 broadening of the most prominent peak in the XRD profile [36]. The crystal phase of  
20  
21 229 Fe<sub>3</sub>O<sub>4</sub> MNPs, SiO<sub>2</sub>@ Fe<sub>3</sub>O<sub>4</sub> MNPs and IL- SiO<sub>2</sub>@ Fe<sub>3</sub>O<sub>4</sub> MNPs were investigated by  
22  
23  
24 230 XRD (as shown in Fig. 3). In the 2θ range of 10–80°, the X-ray diffraction peaks for  
25  
26 231 Fe<sub>3</sub>O<sub>4</sub> (2θ= 30.1°, 35.5°, 43.1°, 53.4°, 57.0°, and 62.6°) were observed on all the three  
27  
28  
29 232 samples, and the peaks positions were indexed as (220), (311), (400), (422), (511),  
30  
31 233 and (440), respectively (JCPDS Card: 019-0629). The XRD patterns showed a good  
32  
33  
34 234 identity with the standard Fe<sub>3</sub>O<sub>4</sub> structure which proved that the particles had got  
35  
36 235 phase stability and the integrity of the structure. The broad peak from 2θ=20° to  
37  
38  
39 236 30° could be seen obviously after coating the particles with silica. It was consistent  
40  
41 237 with an amorphous silica phase in the shell of the silica-coated Fe<sub>3</sub>O<sub>4</sub> nanoparticles  
42  
43  
44 238 [33,37]. No obvious difference was observed between the XRD spectra of  
45  
46 239 SiO<sub>2</sub>@Fe<sub>3</sub>O<sub>4</sub> MNPs and IL- SiO<sub>2</sub>@Fe<sub>3</sub>O<sub>4</sub> MNPs except that the intensity of the XRD  
47  
48  
49 240 peaks decreased, which resulted from the preferred orientation of crystalline faces  
50  
51 241 [35]. This result of the XRD spectra indicated that the crystal phase of Fe<sub>3</sub>O<sub>4</sub>  
52  
53  
54 242 nanoparticle was not changed during the coating process.

55  
56 243 The intensity of magnetism was important for magnetic materials to possess  
57  
58  
59  
60

1  
2  
3  
4 244 sufficient magnetic properties in separation from liquid medium. VSM was used to  
5  
6 245 evaluate the magnetization of the MNPs. Fig. 4a shows the VSM magnetization  
7  
8  
9 246 curves of Fe<sub>3</sub>O<sub>4</sub> MNPs, SiO<sub>2</sub>@Fe<sub>3</sub>O<sub>4</sub> MNPs and IL- SiO<sub>2</sub>@Fe<sub>3</sub>O<sub>4</sub> MNPs at room  
10  
11 247 temperature. It was found that the saturation magnetization of Fe<sub>3</sub>O<sub>4</sub> MNPs and  
12  
13  
14 248 SiO<sub>2</sub>@Fe<sub>3</sub>O<sub>4</sub> MNPs were 71.87 emu g<sup>-1</sup> and 37.40 emu g<sup>-1</sup>, respectively.

15  
16 249 The saturation magnetization of SiO<sub>2</sub>@Fe<sub>3</sub>O<sub>4</sub> MNPs decreased in comparison  
17  
18  
19 250 with Fe<sub>3</sub>O<sub>4</sub> MNPs which was likely resulted from the nonmagnetic silica coating shell.  
20  
21 251 The saturation magnetization has a slight decrease after modified ionic liquids on the  
22  
23  
24 252 magnetic nanoparticles. Nevertheless, the saturation magnetization value of 37.40  
25  
26 253 emu g<sup>-1</sup> for the IL-SiO<sub>2</sub>@Fe<sub>3</sub>O<sub>4</sub>MNPs was high enough to make them easily and  
27  
28  
29 254 quickly separate from the suspension (as shown in Fig. 4b).

30  
31 255 The microscopic structure of the particle was observed by transmission electron  
32  
33  
34 256 microscopy (TEM). Fig. 5a and 5b illustrated that the naked of Fe<sub>3</sub>O<sub>4</sub> particles had a  
35  
36  
37 257 mean diameter of about 20 -30nm. Fig. 5c and 5d showed the Fe<sub>3</sub>O<sub>4</sub>particles coated  
38  
39 258 by silica which had uniform size about 300-400 nm. Moreover, the dark SiO<sub>2</sub>@Fe<sub>3</sub>O<sub>4</sub>  
40  
41 259 MNPs surrounded by a gray liquid could be observed in Fig. 5e after modified with  
42  
43  
44 260 ionic liquids which might be because of the layer of ionic liquids surrounding. It can  
45  
46  
47 261 be observed that all of particles appear to be roughly spherical in shape which were  
48  
49 262 homogeneous, monodisperse, and spherical.

### 50 51 263 **3.2 MSPE of different ionic liquid and different protein**

52  
53  
54 264 Five kinds of ionic liquids with the common anion of chloride modified on the  
55  
56  
57 265 surface of magnetic nanoparticles have been investigated for the extraction of three  
58  
59  
60

1  
2  
3  
4 266 proteins (BSA, BHB, OVA). The extraction efficiencies were shown in supplementary  
5  
6 267 data Table S2. As an example, the values of the extraction efficiencies for BSA  
7  
8 268 change from 47.21% to 18.46%. It is clear that the hydroxyl ammonium-based IL has  
9  
10  
11 269 a higher extraction efficiency, and the poorest effect is shown by the  
12  
13  
14 270 guanidinium-based ionic liquid.

15  
16 271 Because the ionic liquids have a wide structural diversity, the extraction  
17  
18 272 efficiency was also differences. It can be seen from Fig. 6, the [Simam][Cl] modified  
19  
20  
21 273 on the surface of magnetic nanoparticles has a higher extraction rate than others, it  
22  
23  
24 274 may be attributed to the hydrogen bond interaction between the hydroxyl of the IL  
25  
26 275 cation and the aliphatic hydrocarbon residue of the protein. Therefore, magnetic  
27  
28  
29 276 solid-phase extraction based on hydroxy functional ionic liquid modified on the  
30  
31 277 surface of silica-coated magnetic  $\text{Fe}_3\text{O}_4$  ([Simam][Cl]-MNPs) was selected and take  
32  
33  
34 278 BSA as the object for the following study.

### 35 36 279 **3.3 Optimization of MSPE parameters**

#### 37 38 39 280 **3.3.1 Effect of the amount of [Simam][Cl]-MNPs**

40  
41 281 In order to discuss the effect on extraction efficiency of the mass of IL-MNPs, a  
42  
43 282 specific mass of [Simam][Cl]-MNPs and protein solution ( $0.5 \text{ g mL}^{-1}$  and  $2.0 \text{ mL}$ )  
44  
45  
46 283 systems were adopted, then the suspension was immediately stirred for 30 min at  
47  
48  
49 284  $30 \text{ }^\circ\text{C}$  and the results were illustrated in Fig. 7a. We can see that the extraction  
50  
51 285 efficiency was increased with the addition of IL-MNPs. The reason could be that the  
52  
53  
54 286 more number of [Simam][Cl]-MNPs is, the more adsorption sites would be available  
55  
56  
57 287 for protein molecules adsorbed. The extraction efficiency of BSA has been reached  
58  
59  
60

1  
2  
3  
4 288 81.33% when the mass of [Simam][Cl]-MNPs was 60 mg. The extraction efficiency  
5  
6 289 was not obviously increased when the amount of [Simam][Cl]-MNPs attained 70 mg.  
7  
8  
9 290 So 60 mg of [Simam][Cl]-MNPs was chosen in next experiment.

### 291 **3.3.2 Effect of the mass of protein**

292 To study the effect of sample concentration on the extraction efficiency of  
293 [Simam][Cl]-MNPs, a series of concentration of protein solutions (0.50-1.75 mg mL<sup>-1</sup>)  
294 were examined at 30 °C and shaken for 30 min. From Fig. 7b, it can be seen that with  
295 the increase in concentration of BSA, the extraction yield decreased correspondingly.  
296 This observation can be explained by this fact that an extraction system has a limited  
297 ability of extraction when the number of adsorbent was the same. So the system is  
298 near saturation when the concentration of BSA addition is more than 0.5 mg mL<sup>-1</sup> the  
299 extraction quantity may have a little increase, but the extraction efficiency decreases  
300 rapidly. According to the above result, 0.5 mg mL<sup>-1</sup> BSA solution was selected.

### 301 **3.3.3 Effect of solution pH**

302 Owing to the proteins as amphoteric molecules, the effect of the initial pH of the  
303 solution on the adsorption of proteins onto IL-MNPs surfaces was studied. A series of  
304 pH range from 3.0 to 9.0 of protein solutions (0.5 mg mL<sup>-1</sup>, 2.0 mL) were examined.  
305 60 mg of [Simam][Cl]-MNPs was added and shaken for 30 min at 30 °C. The results  
306 are depicted in Fig. 7c. The extraction yields of BSA was relatively high at pH=6. This  
307 may be associated with the following reason. The isoelectric point of BSA is about  
308 4.7–5.2 and consequently a net charge of almost zero is expected for it at about pH  
309 5.0[6]. At pH = 6, BSA has negative charges and the surfaces of IL-MNPA

1  
2  
3  
4 310 nanoparticles are positive [7]. The pH value was adjusted to make a strong  
5  
6 311 electrostatic attraction between negatively-charged BSA and positively-charged  
7  
8  
9 312 nanoparticles. Based on these results, a pH value of 6.0 was selected in order to  
10  
11 313 perform next investigations.

#### 12 13 14 314 **3.3.4 Effects of extraction time**

15 The effect of the extraction time in MSPS was investigated by changing the  
16  
17 316 shaking time. From Fig. 7d, it can be seen that the extraction efficiency of BSA  
18  
19 317 increased rapidly in the first 20 min, and over 20 min the extraction efficiency had  
20  
21 318 almost reached the maximum. It can be speculated that when the extraction process is  
22  
23 319 just beginning, there are many adsorption sites on the surface of the  
24  
25 320 [Simam][Cl]-MNPs which would be available for protein molecules adsorbed, so the  
26  
27 321 extraction capacity increases quickly. With the growth of time, more and more  
28  
29 322 adsorption sites were occupied and the extract speed gradually slows down until  
30  
31 323 extraction reached equilibrium.

#### 32 324 **3.3.5 Effect of solution temperature**

33 To further confirm the temperature range to the influence of extraction efficiency,  
34  
35 326 a series of experiments were performed over a temperature range of 20–70 °C. Sixty  
36  
37 327 milligram of [Simam][Cl]-MNPs and 2.0 mL of 0.5 mg mL<sup>-1</sup> protein solution at pH =  
38  
39 328 6 were used. In light of Fig. 7e, as the temperature increased from 20 to 30 °C, the  
40  
41 329 extraction efficiency of the protein increased with the increasing temperature. But the  
42  
43 330 temperature kept at 30 °C or higher, the extraction yield decreased correspondingly.  
44  
45 331 The possible reason for this phenomenon was that the adsorption process of protein  
46  
47 332 onto the [Simam][Cl]-MNPs was endothermic process. But when the temperature  
48  
49 333 continues to rise, the extraction rate was reduced. It means that the temperature was  
50  
51  
52  
53  
54  
55  
56  
57  
58  
59  
60



1  
2  
3  
4 334 high to destroy the hydrogen bonding interaction between the ionic liquids modified  
5  
6 335 on the surface of magnetic nanoparticles and the surface water of protein's amino acid  
7  
8  
9 336 residue. Through further study found that when the temperature exceeds 60 °C, BSA  
10  
11 337 was denaturated. So the extraction was carried out at 30 °C because of the relatively  
12  
13 338 high extraction yield. All single-factor experimental data were summarized in  
14  
15  
16 339 supplementary data Table S3.

### 18 19 340 **3.4 Methodological study**

20  
21 341 Under the optimized extraction conditions, a series of experiments were  
22  
23 342 performed to validate the developed MSPE method for three times by UV detection.  
24  
25 343 Apparatus precision was investigated by the analysis of the solution of BSA for three  
26  
27 344 times. The RSD obtained was 0.55%. The result indicates that the precision of the  
28  
29 345 UV-vis spectra is great. Three copies of the same sample measured respectively under  
30  
31 346 the same conditions. The calculation of RSD was 1.47% (n=3) which indicate that this  
32  
33 347 method has excellent repeatability. Taking a sample detected continuously in three  
34  
35 348 days under the same conditions to verify the stability experiment. The result of the  
36  
37 349 RSD was 1.27% (n=3), which explain that the sample is recoverable within three days  
38  
39 350 (as shown in supplementary data Table S4) .

### 40 41 351 **3.5 Desorption studies**

42  
43 352 The regeneration of protein is an important factor to be reported for potential  
44  
45 353 applications. Different concentrations of NaCl (2.0 mL) was used and the possible  
46  
47 354 desorption of proteins (0.5 mg mL<sup>-1</sup> protein already adsorbed on 60 mg  
48  
49 355 [Simam][Cl]-MNPs under optimum extraction conditions) was added. It can be seen  
50  
51  
52  
53  
54  
55  
56  
57  
58  
59  
60

1  
2  
3  
4 356 from Fig. 8 that with the increasing of the concentration of NaCl, the percentage of  
5  
6 357 BSA desorbed increased and the desorption ratios reached 95.34% when the  
7  
8  
9 358 concentrations of NaCl greater than 1.1 mol L<sup>-1</sup>. The results showed that the adsorbed  
10  
11 359 BSA could be easily desorpted from [Simam][Cl]-MNPs.

### 14 360 **3.6 Regeneration of the IL-MNPs**

16 361 To evaluate the sorbent performance, regeneration is a key factor for making  
17  
18 362 the process economic and environmental protection. Nearly 95% of  
19  
20 363 [Simam][Cl]-MNPs could be recovered from each run. Finally, several consecutive  
21  
22 364 adsorption–desorption cycles were performed and the result showed in supplementary  
23  
24 365 data Fig S2. In a test of four cycles, the [Simam][Cl]-MNPs could be reused and the  
25  
26 366 extraction efficiency was about 84.35 -82.64 % which without any significant loss of  
27  
28 367 the extraction efficiency. These results revealed that the sorbent was excellent stable  
29  
30 368 and could endure these reaction conditions. But after five runs a 24.16% decrease in  
31  
32 369 its performance was observed. The reason of the limited reusable times may have the  
33  
34 370 following points. On the one hand, the mass of magnetic nanoparticles will be lost  
35  
36 371 after many times regeneration. Because the adsorbents was be weight for one time and  
37  
38 372 washed many time by ethanol and water in the recycling and reusing test. On the other  
39  
40 373 hand, the mass of ionic liquid modified on the surface of magnetic nanoparticles will  
41  
42 374 become less and it is dissolved in solution after wash many time by ethanol and water.  
43  
44 375 The all will lead to a decline of the extraction rate. Therefore the reuse limit of the  
45  
46 376 proposed sorbent was five cycles.  
47  
48  
49  
50  
51  
52  
53  
54  
55  
56  
57  
58  
59  
60

### 378 3.7 Comparison with other methods

379 Protein can easily be extracted from the mixture through the traditional liquid-liquid  
380 extraction process, but it is hard to recycle from the extract. Compared with  
381 traditional liquid-liquid extraction method, solid phase extraction has many  
382 advantages such as low consumption of organic solvents, high recovery and reuse rate.  
383 Magnetic solid phase extraction is an emerging technology for pretreating samples in  
384 recent years. It put together liquid-solid extraction and magnetic properties. A novel  
385 form of traditional SPE, the magnetic sorbents are easily collected and separated from  
386 the solution with an external magnetic field which are convenient, time and effort  
387 saving.

388 We know that C18 has a wide range of applications in the separation of mixture. But  
389 the ionic-liquid coated magnetic particles has some advantages which the C18 do not  
390 have. For example, the greatest feature of ionic liquids is designing. By adjusting the  
391 combination or introducing an appropriate functional groups, the specific ionic liquids  
392 can be obtained. In addition, the hydroxy functional ionic liquids modified magnetic  
393 nanoparticles have the potential to extract protein from water samples based on  
394 hydrogen bond and electrostatic interaction between the ionic liquid and protein  
395 which C18 haven't. So this is more conducive to the selective separation of proteins.  
396 Considering the results, the sorbent prepared in this study possesses many advantages  
397 which is proved to be an efficient, reliable and convenient material for the extraction  
398 of protein from water samples.

399

#### 400 **4. Conclusions**

401 This paper systematically investigated the extraction efficiency of protein based  
402 on a novel magnetic nanoparticles which was fabricated by modifying hydroxy  
403 functional ionic liquid on the surface of silica-coated magnetic Fe<sub>3</sub>O<sub>4</sub> (IL-MNPs).  
404 Some parameters such as the mass of IL-MNPs, the protein concentration, pH of  
405 solution and temperature were optimized and under the optimal conditions, 86.92% of  
406 BSA was extracted. The high adsorption capacity, short contact time, stability, low  
407 aggregation, reusability, and selective adsorption ability are the advantages of  
408 hydroxy functional ionic liquid modified on the surface of silica-coated magnetic  
409 Fe<sub>3</sub>O<sub>4</sub> nanoparticles as adsorbent compared with traditional extraction materials. The  
410 performances of the method indicate that it have the potential to offer new possibility  
411 in the extraction of bio-analysis and proved that [Simam][Cl]-MNPs can be an  
412 important tool in bio-separation technology as well as other biotechnological  
413 applications.

#### 414 **Acknowledgements**

415 The authors greatly appreciate the financial supports by the National Natural  
416 Science Foundation of China (No. 21175040; No. 21375035; No.J1210040) and the  
417 Foundation for Innovative Research Groups of NSFC (Grant 21221003).

418  
419  
420  
421

422 **References**

- 423 [1] Y. Pei, J. Wang, K. Wu, X. Xuan and X. Lu, *Sep. Purif. Technol.*, 2009, 64, 288-295.
- 424 [2] A. R. Piergiovanni, *J. Agric. Food Chem.*, 2007, 55, 3850-3856.
- 425 [3] E. Zatloukalova and Z. Kucerova, *J. Chromatogr. B*, 2004, 808, 99-103.
- 426 [4] X. Lin, Y. Z. Wang, Z. Qun, X. Q. Ding and J. Chen, *Analyst*, 2013, 138, 6445-6453.
- 427 [5] Q. Zeng, Y. Z. Wang, N. Li, X. Huang, X. Q. Ding and X. Lin, *Talanta*, 2013, 116, 409-416.
- 428 [6] S. Kamran, M. Asadi and G. Absalan, *Microchim Acta*, 2013, 180, 41-48.
- 429 [7] G. Absalan, M. Asadi, S. Kamran, L. Sheikhan, D. M. Goltz, *J. Hazard. Mater.*, 2011, 192, 476-484.
- 430 [8] M. H. Liao and D. H. Chen, *Biotechnology Letters*, 2002, 24, 1913-1917.
- 431 [9] Y. Zou, Y. Z. Chen, Z. H. Yan, C. Y. Chen, J. P. Wang and S. Z. Yao, *Analyst*, 2013, 138,
- 432 5904-5912.
- 433 [10] L. Xiong, H. W. Jiang and D. Z. Wang, *Acta. Polymerica. Sinica*, 2008, 3, 259-265.
- 434 [11] F. Bianchi, V. Chiesi, F. Casoli, P. Luches, L. Nasi, M. Careri and A. Mangia, *J. Chromatogr. B*,
- 435 2012, 1231, 8-15.
- 436 [12] S. X. Zhang, H. Y. Niu, Y. Y. Zhang, J. S. Liu, Y. L. Shi, X. L. Zhang and Y. Q. Cai, *J.*
- 437 *Chromatogr. A*, 2012, 1238, 38-45.
- 438 [13] P. Walden, *Bull Acad Imperial Sci*, 1941, 1800, 405-422.
- 439 [14] P. Sun and D. W. Armstrong, *Analytica Chimica Acta*, 2010, 661, 1-6.
- 440 [15] D. Xiao, D. H. Yuan, H. He, *Carbon*, 2014, 274-286.
- 441 [16] H. He, D. H. Yuan, Z. Q. Gao, *J. Chromatography. A*, 2014, 1324, 78-85.
- 442 [17] Y. Sha, C. Deng and B. Liu, *J. Chromatogr. A*, 2008, 27, 1198-1199.
- 443 [18] Y. Y. Jiang, C. Guo, H. S. Xia, I. Mahmood, C. Z. Liu and H. Z. Liu, *J. Molecular Catalysis B:*

- 1  
2  
3  
4 444 Enzymatic, 2009, 58, 103-109.  
5  
6 445 [19] M. Ghaemi and G. Absalan, *Microchim Acta*, 2013, 158, 521-530.  
7  
8 446 [20] M. H. Mashhadizadeh and Z. Karami, *J. Hazard. Mater.*, 2011, 190, 1023-1029.  
9  
10 447 [21] Y. Liu, H. Li and J.M. Lin, *Talanta*, 2009, 77, 1037-1042.  
11  
12 448 [22] L. Bai, B. Mei, Q.Z. Guo, Z.G. Shi and Y.Q. Feng, *J. Chromatogr. A*, 2010, 1217, 7331-7336.  
13  
14 449 [23] S. Zhang, H. Niu, Y. Cai and Y. Shi, *J. Chromatogr. A*, 2010, 1217, 4757-4764.  
15  
16 450 [24] S. Zhang, H. Niu, Y. Cai and Y. Shi, *Anal. Chim. Acta*, 2010, 665, 167-175.  
17  
18 451 [25] M. Bouri, M. Gurau, M. Zougagh and Á. Rios, *Anal Bioanal Chem*, 2012, 404, 1529-1538.  
19  
20 452 [26] B. Tural, T. Tarhan, S. Tural, *Journal of Molecular Catalysis B: Enzymatic*, 2014, 102, 188–194.  
21  
22 453 [27] B. Tural, S. Tural, A.S. Demir, *Journal of Molecular Catalysis. B, Enzymatic*, 2013, 95, 41-47.  
23  
24 454 [28] B. Tural, S. Tural, A.S. Demir, *Chirality*, 2013, 25, 415-421.  
25  
26 455 [29] B. Tural, I. Simsek, S. Tural, A. S. Demir, *Tetrahedron: Asymmetry* 2013, 24, 260–268.  
27  
28 456 [30] J. Wang, B. L. Xu, H. Y. Sun and G. H. Song, *Tetrahedron Letters* 2013, 54, 238-241.  
29  
30 457 [31] R. A. Reziq, D. S. Wang, M. Post and H. Alpera, *Adv. Synth. Catal*, 2007, 349, 2145-2150.  
31  
32 458 [32] A. K. Nezhad and S. Mohammadi, *American Chemical Society*, 2013, 15, 512-518.  
33  
34 459 [33] Q. Zhang, H. Su, J. Luo and Y. Y. Wei, *Green Chemistry*, 2012, 14, 201-208.  
35  
36 460 [34] P. Wang, A. G. Kong, W. J. Wang, H. Y. Zhu and Y. K. Shan, *Catal Lett*, 2010, 135, 159-164.  
37  
38 461 [35] X. P. Jia, M. L. Xu, Y. Y. Wang, D. Ran, S. Yang and M. Zhang, *Analyst*, 2013, 138, 651-659.  
39  
40 462 [36] M. Faraji, Y. Yamini and M. Rezaee, *J. Iran. Chem. Soc.*, 2010, 7, 1-37.  
41  
42 463 [37] P. Sun and D. W. Armstrong, *Analytica Chimica Acta*, 2010, 661, 1-16.  
43  
44 464  
45  
46 465  
47  
48 466  
49  
50  
51  
52  
53  
54  
55  
56  
57  
58  
59  
60

467

468 **Table 1 The types of ILs**

ILs	Cation	Anion
[Simam][Cl]		Cl <sup>-</sup>
[Simim][Cl]		Cl <sup>-</sup>
[Siemp][Cl]		Cl <sup>-</sup>
[Sitmg][Cl]		Cl <sup>-</sup>
[Simpv][Cl]		Cl <sup>-</sup>

469

470

471

472

473

474

475

476

477

478

479

480

481

482

483

1  
2  
3  
4  
5  
6  
7  
8  
9  
10  
11  
12  
13  
14  
15  
16  
17  
18  
19  
20  
21  
22  
23  
24  
25  
26  
27  
28  
29  
30  
31  
32  
33  
34  
35  
36  
37  
38  
39  
40  
41  
42  
43  
44  
45  
46  
47  
48  
49  
50  
51  
52  
53  
54  
55  
56  
57  
58  
59  
60

### 484 485 **Figure captions**

486 Scheme. 1 Schematic diagram of the synthesis and surface modification of  $\text{Fe}_3\text{O}_4$   
487 magnetic nanoparticles coated with silica ( $\text{SiO}_2@ \text{Fe}_3\text{O}_4$ ) for investigation of proteins  
488 by magnetic solid phase extraction

489 Scheme. 2 Schematic diagram of the synthesis five different ionic liquids at the  
490 surface of magnetic nanoparticles ( $\text{IL-SiO}_2@ \text{Fe}_3\text{O}_4$ )

491 Scheme. 3 The schematic charts of extraction proteins by magnetic solid phase  
492 extraction

493 Fig. 1 The FT-IR spectra of the magnetic nanoparticles and the five ionic liquids

494 modified on MNPs. (a)  $\text{Fe}_3\text{O}_4$  MNPs; (b)  $\text{SiO}_2@ \text{Fe}_3\text{O}_4$  MNPs; (c)

495  $[\text{Simim}][\text{Cl}]\text{-MNPs}$ ; (d)  $[\text{Siemp}][\text{Cl}]\text{-MNPs}$ ; (e)  $[\text{Simpy}][\text{Cl}]\text{-MNPs}$ ; (f)

496  $[\text{Sitmg}][\text{Cl}]\text{-MNPs}$ ; (g)  $[\text{Simam}][\text{Cl}]\text{-MNPs}$

497 Fig. 2 The TGA analysis of (a)  $\text{Fe}_3\text{O}_4$  MNPs; (b)  $\text{SiO}_2@ \text{Fe}_3\text{O}_4$  MNPs; (c)

498  $[\text{Simam}][\text{Cl}]\text{-SiO}_2@ \text{Fe}_3\text{O}_4$  MNPs

499 Fig. 3 The XRD patterns of (a)  $\text{Fe}_3\text{O}_4$  MNPs; (b)  $\text{SiO}_2@ \text{Fe}_3\text{O}_4$  MNPs; (c)

500  $[\text{Simam}][\text{Cl}]\text{-SiO}_2@ \text{Fe}_3\text{O}_4$  MNPs

501 Fig. 4 The VSM analysis of A(a)  $\text{Fe}_3\text{O}_4$  MNPs; A(b)  $\text{SiO}_2@ \text{Fe}_3\text{O}_4$  MNPs; A(c)

502  $[\text{Simam}][\text{Cl}]\text{-SiO}_2@ \text{Fe}_3\text{O}_4$  MNPs, and the magnetic response of

503  $[\text{Simam}][\text{Cl}]\text{-MNPs}$  to external magnetic field (B)

504 Fig. 5 The micro-pictures of (a), (b)  $\text{Fe}_3\text{O}_4$  MNPs (TEM); (c), (d)  $\text{SiO}_2@ \text{Fe}_3\text{O}_4$

505 MNPs(TEM); (e)  $[\text{Simam}][\text{Cl}]\text{-SiO}_2@ \text{Fe}_3\text{O}_4$  MNPs (TEM)

506 Fig. 6 Five kinds of ionic liquids modified magnetic nanoparticles were been

507 investigated for the extraction of three proteins (a)BSA, (b)BHb, (c)OVA and



1  
2  
3  
4 508 (d) [Simam][Cl]-MNPs extraction of three proteins, respectively.  
5

6 509 Fig. 7 Single factor experiments: (a) the mass of [Simam][Cl]-MNPs; (b) protein  
7  
8  
9 510 concentration;(c) the solution pH;(d) the extraction time; (e) temperature  
10

11 511 Fig. 8 Desorption BSA from the surfaces of [Simam][Cl]-MNPs experiment.  
12

13 512 Fig. S1 Infrared spectroscopy of ILs: (a) [Simam][Cl]; (b) [Simim][Cl]; (c)  
14  
15  
16 513 [Siemp][Cl]; (d) [Sitmg][Cl]; (e) [Simpy][Cl].  
17

18  
19 514 Fig. S2 Reusing experiment of [Simam][Cl]-MNPs.  
20

21 515

22 516

23 517

24 518

25 519

26 520

27 521

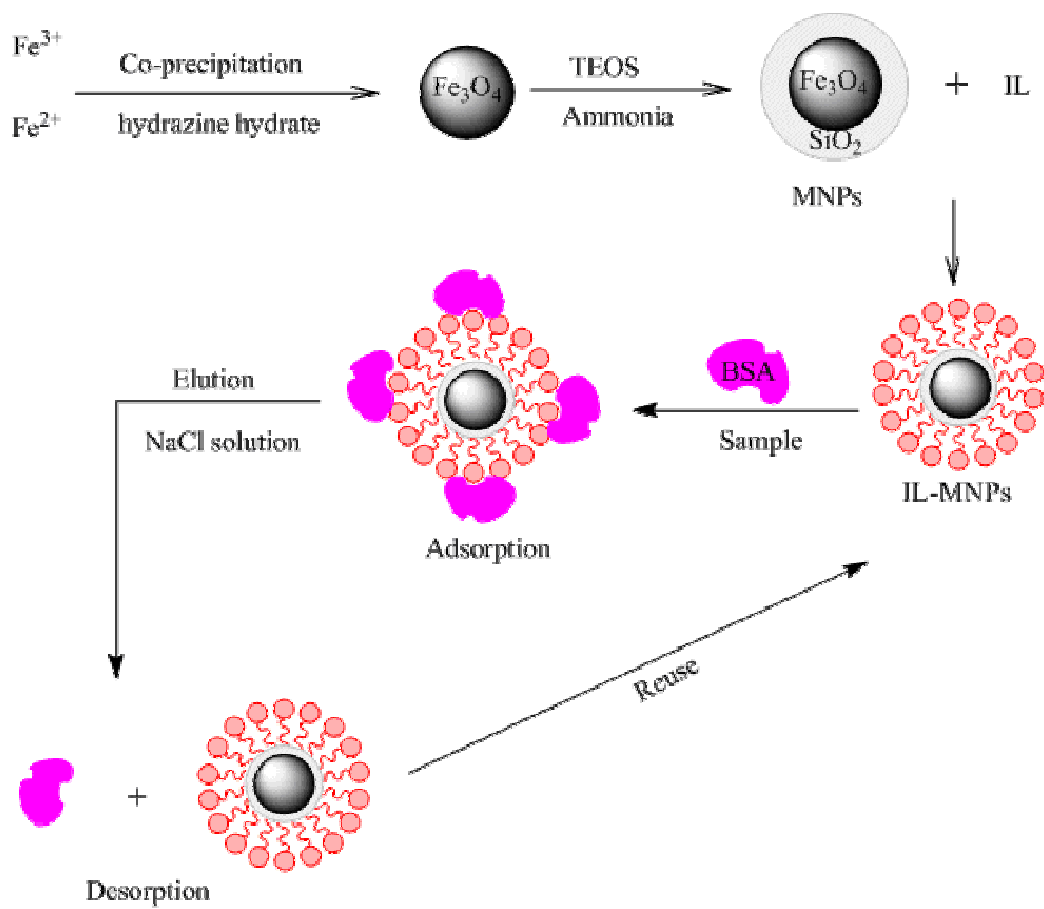
28 522

29 523

30 524

31 525

32  
33  
34  
35  
36  
37  
38  
39  
40  
41  
42  
43  
44  
45  
46  
47  
48  
49  
50  
51  
52  
53  
54  
55  
56  
57  
58  
59  
60



526

527

528

529

530 Scheme. 1 Schematic diagram of the synthesis and surface modification of  $\text{Fe}_3\text{O}_4$ 531 magnetic nanoparticles coated with silica ( $\text{SiO}_2@ \text{Fe}_3\text{O}_4$ ) for investigation of

532 proteins by magnetic solid phase extraction.

533

534

535

536

537

538

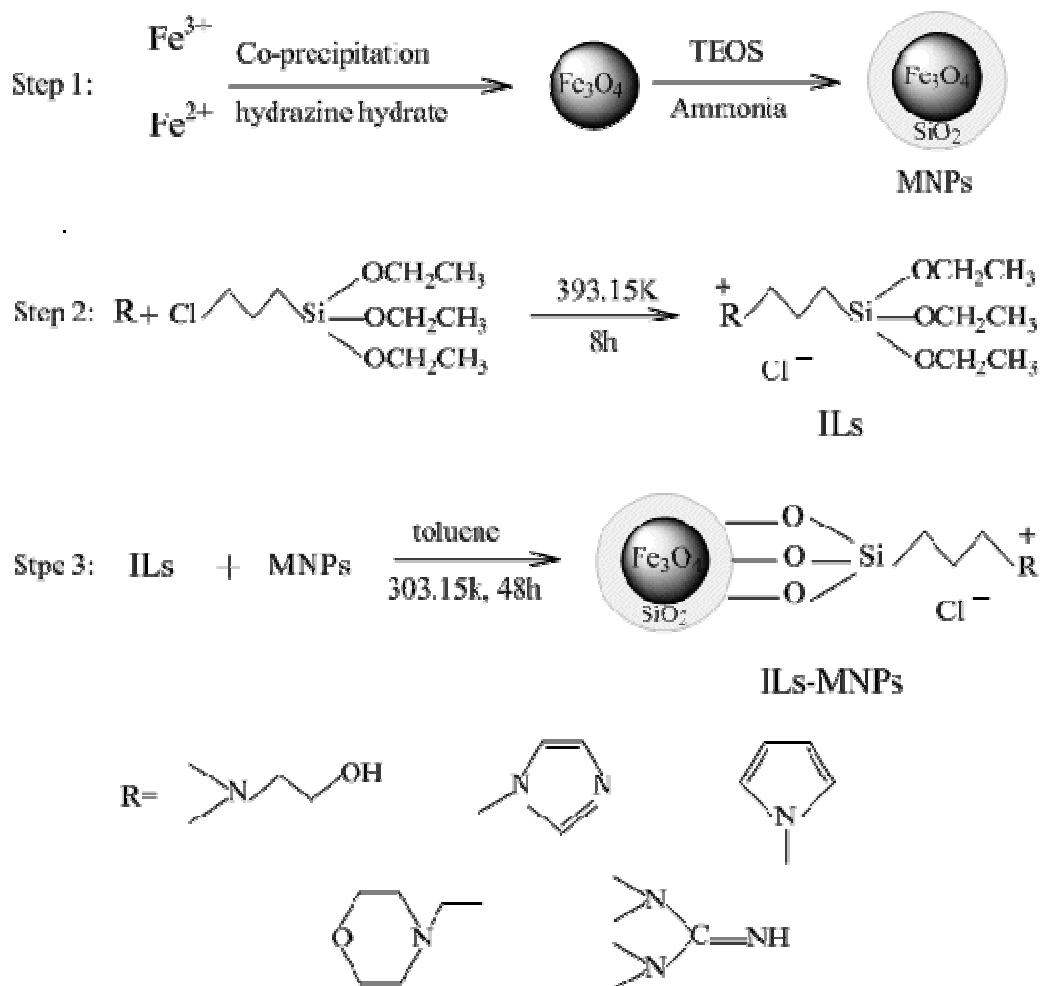
539

540

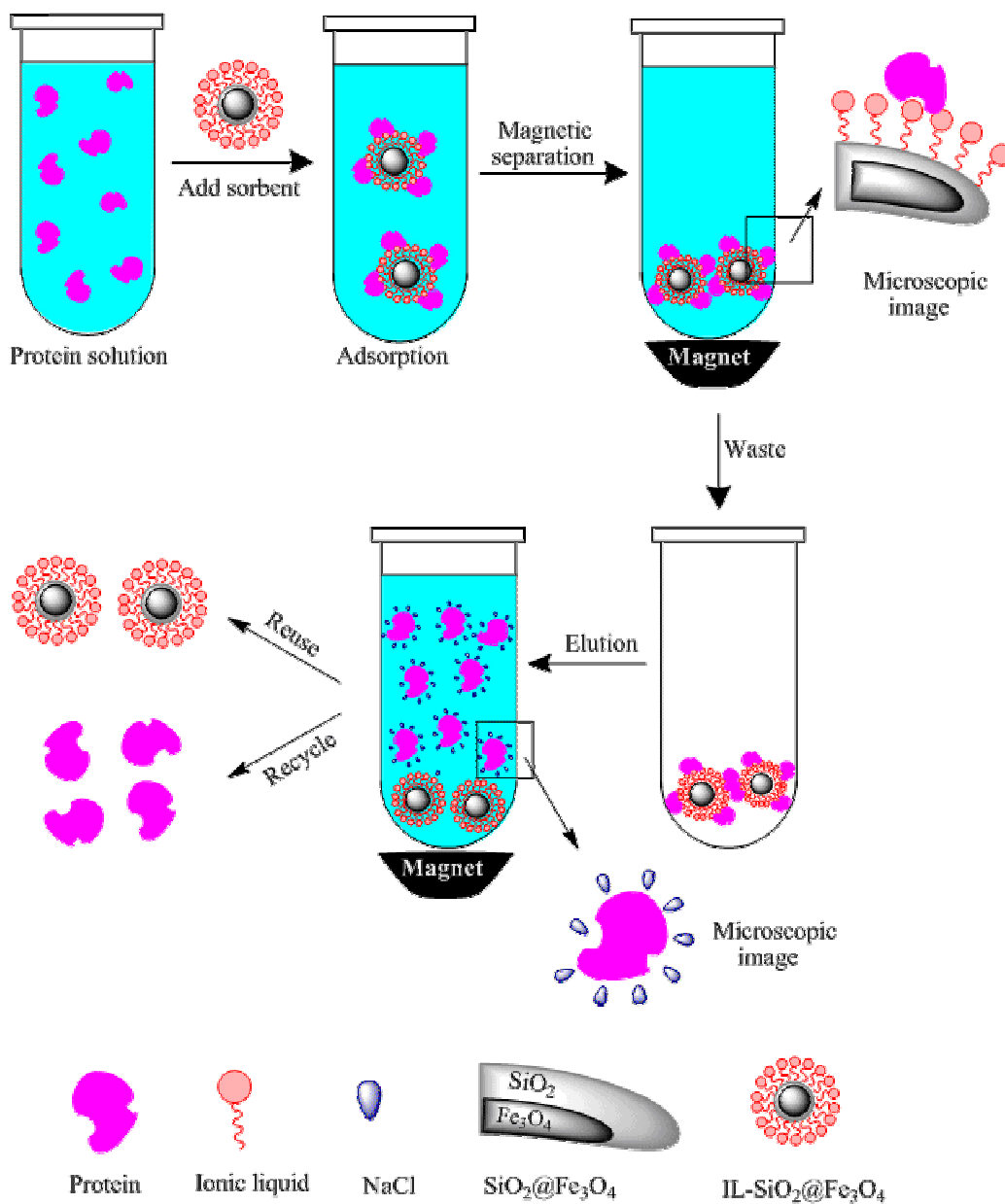
541

542

543



545 Scheme. 2 Schematic diagram of the synthesis five different ionic liquids at the  
546 surface of magnetic nanoparticles (IL-SiO<sub>2</sub>@ Fe<sub>3</sub>O<sub>4</sub>)



560

561

562 Scheme. 3 The schematic charts of extraction proteins by magnetic solid phase

563 extraction.

564

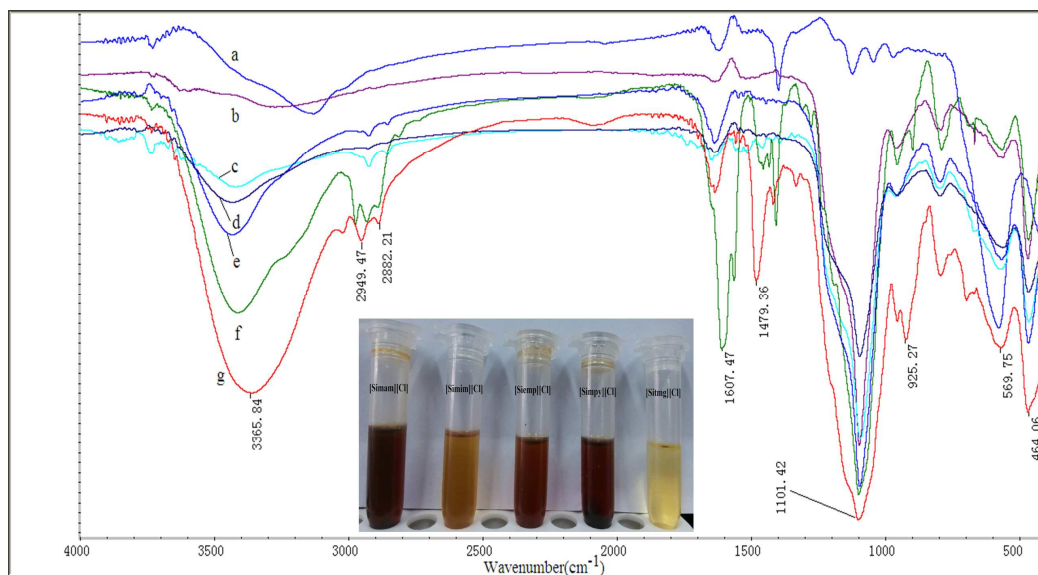
565

566

567

568

569



570

571 Fig. 1 The FT-IR spectra of the magnetic nanoparticles and the five ionic liquids

572 modified on MNPs.(a)  $\text{Fe}_3\text{O}_4$  MNPs; (b)  $\text{SiO}_2@ \text{Fe}_3\text{O}_4$  MNPs; (c)

573 [Simim][Cl]-MNPs; (d) [Siemp][Cl]-MNPs; (e) [Simpj][Cl]-MNPs; (f)

574 [Sitmg][Cl]-MNPs; (g) [Simam][Cl]-MNPs

575

576

577

578

579

580

581

582

583

584

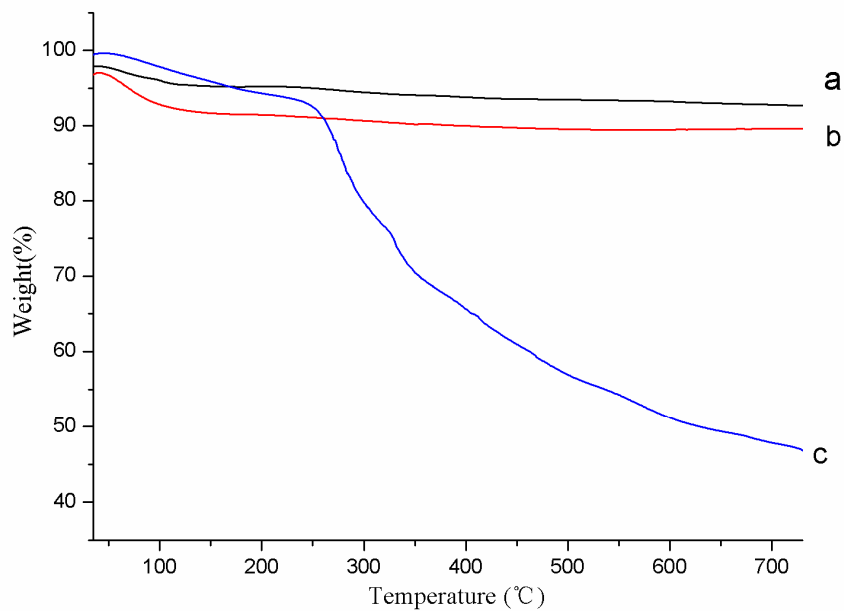
585

586

587

588

589



590

591

Fig. 2 The TGA analysis of (a)  $\text{Fe}_3\text{O}_4$  MNPs; (b)  $\text{SiO}_2@ \text{Fe}_3\text{O}_4$  MNPs; (c)

592

[Simam][Cl]- $\text{SiO}_2@ \text{Fe}_3\text{O}_4$  MNPs

593

594

595

596

597

598

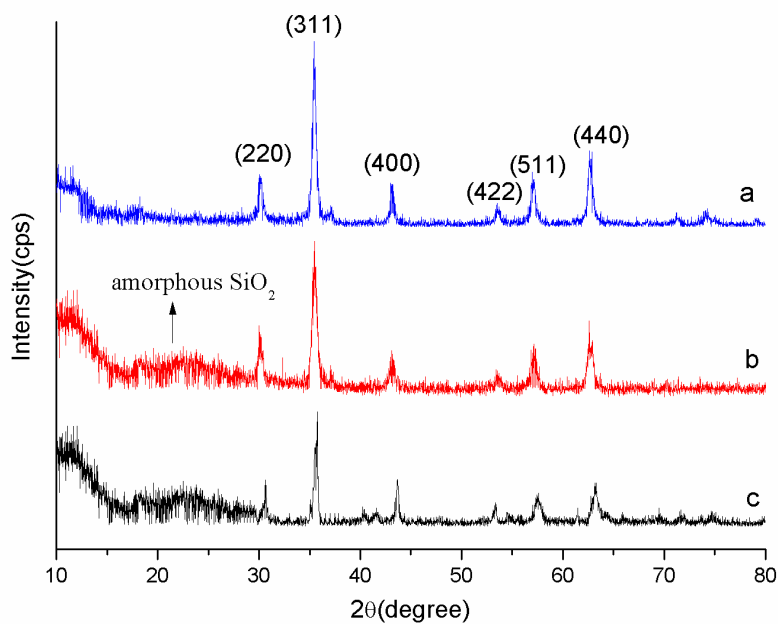
599

600

601

602

603



604

605 Fig. 3 The XRD patterns of (a) Fe<sub>3</sub>O<sub>4</sub> MNPs; (b) SiO<sub>2</sub>@ Fe<sub>3</sub>O<sub>4</sub> MNPs; (c)

606

[Simam][Cl]-SiO<sub>2</sub>@ Fe<sub>3</sub>O<sub>4</sub> MNPs

607

608

609

610

611

612

613

614

615

616

617

618

619

620

621

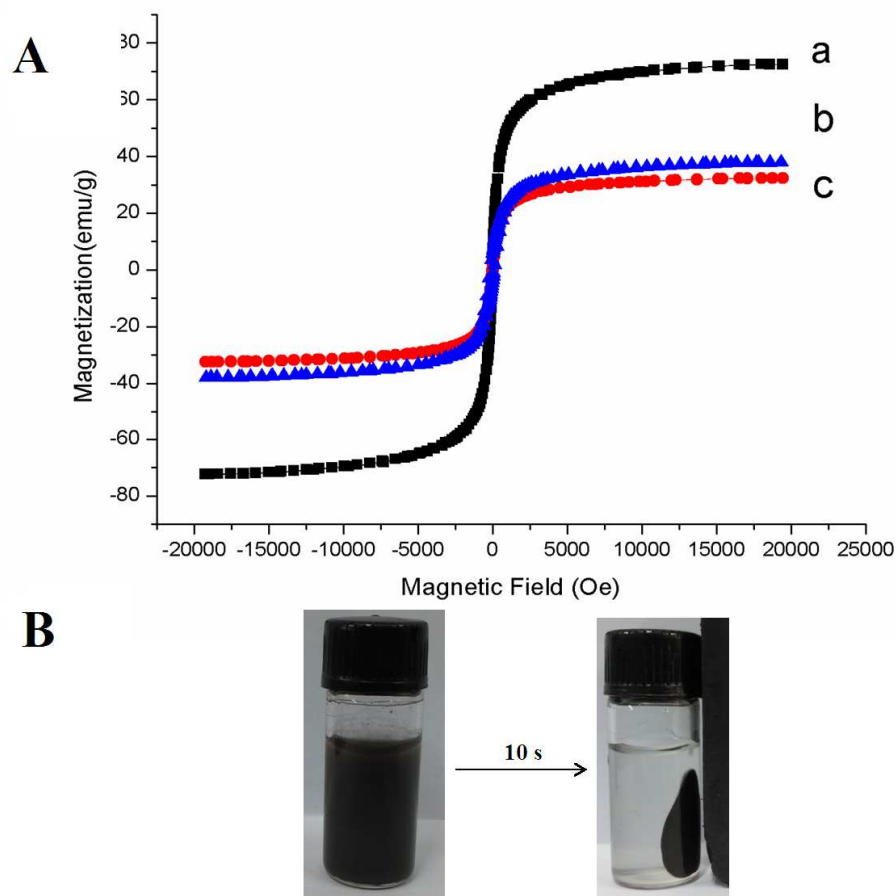
622

623

624

625

626



627

628

629 Fig.4 The VSM analysis of A(a)  $\text{Fe}_3\text{O}_4$  MNPs; A(b)  $\text{SiO}_2@ \text{Fe}_3\text{O}_4$  MNPs; A(c)630 [Simam][Cl]-  $\text{SiO}_2@ \text{Fe}_3\text{O}_4$  MNPs, and the magnetic response of

631 [Simam][Cl]-MNPs to external magnetic field (B)

632

633

634

635

636

637

638

639

640

641

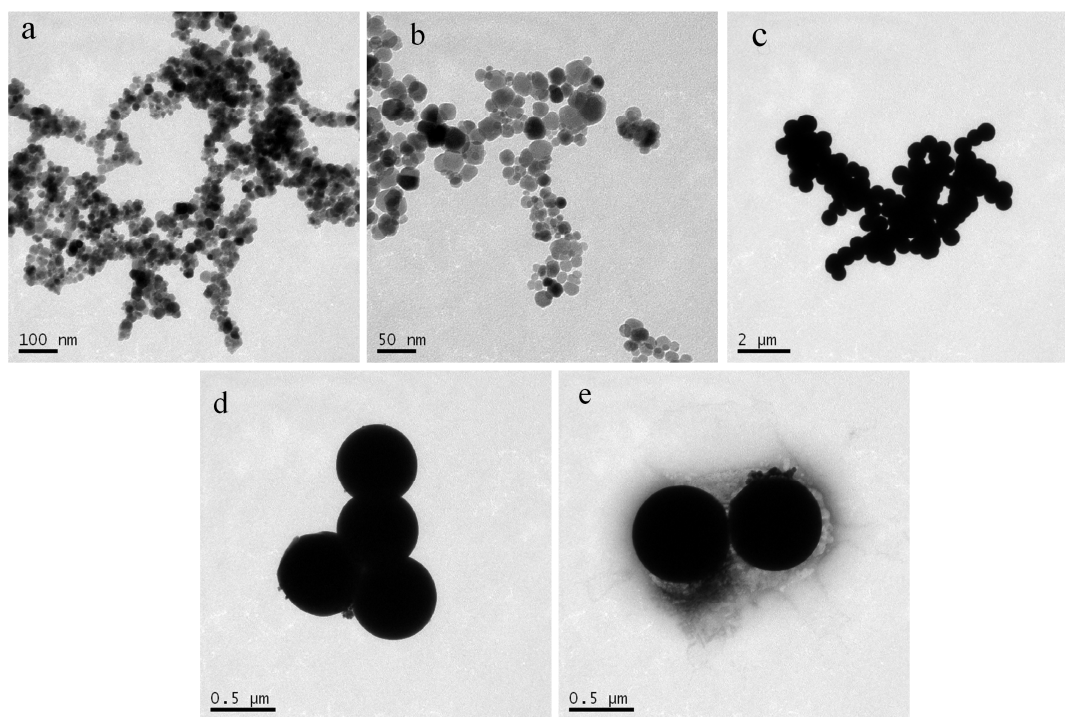
642

643



644

645



646

647

648 **Fig. 5** The micro-pictures of (a), (b)  $\text{Fe}_3\text{O}_4$  MNPs (TEM); (c), (d)  $\text{SiO}_2@ \text{Fe}_3\text{O}_4$ 649 MNPs(TEM); (e) [Simam][Cl]- $\text{SiO}_2@ \text{Fe}_3\text{O}_4$  MNPs (TEM)

650

651

652

653

654

655

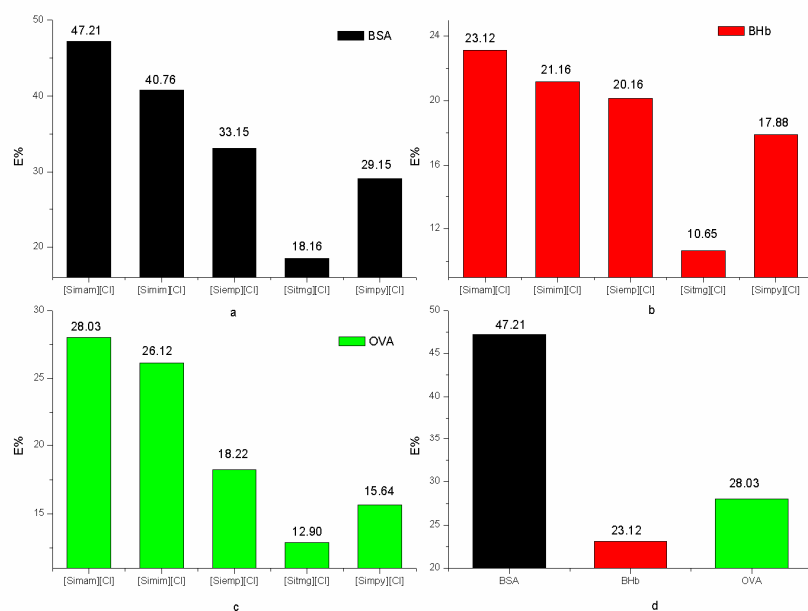
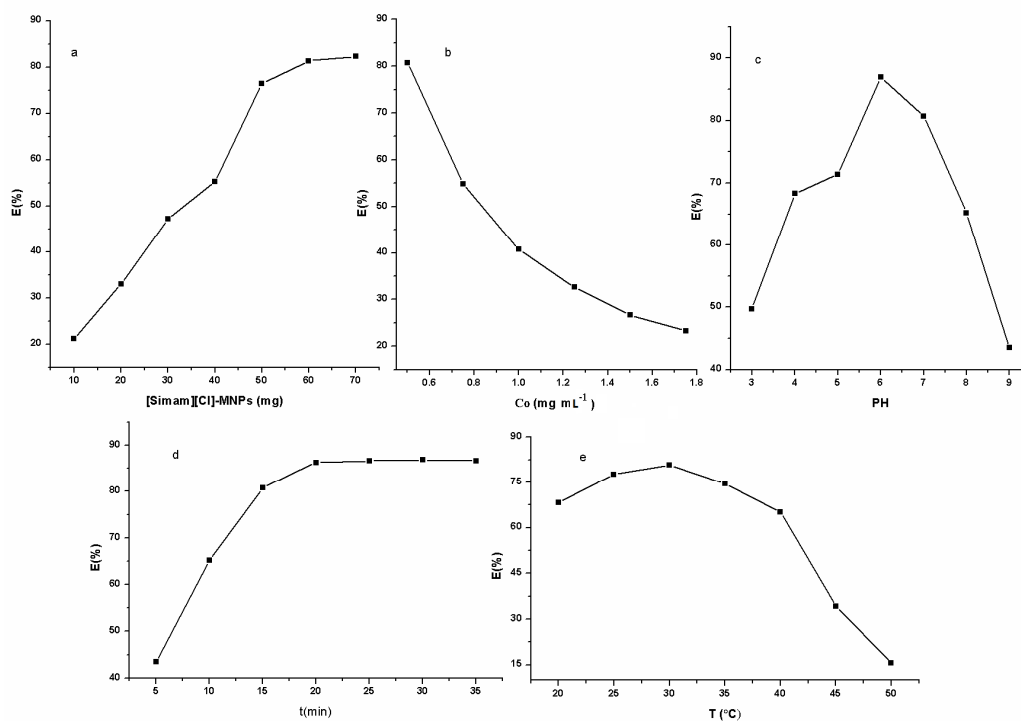


**Fig. 6** Five kinds of ionic liquids modified magnetic nanoparticles were been investigated for the extraction of three proteins (a)BSA, (b)BHb, (c)OVA and (d) [Simam][Cl]-MNPs extraction of three proteins, respectively.

678



679

680 **Fig. 7** Single factor experiments: (a) the mass of [Simam][Cl]-MNPs; (b) protein

681 concentration;(c) the solution pH;(d) the extraction time; (e) temperature

682

683

684

685

686

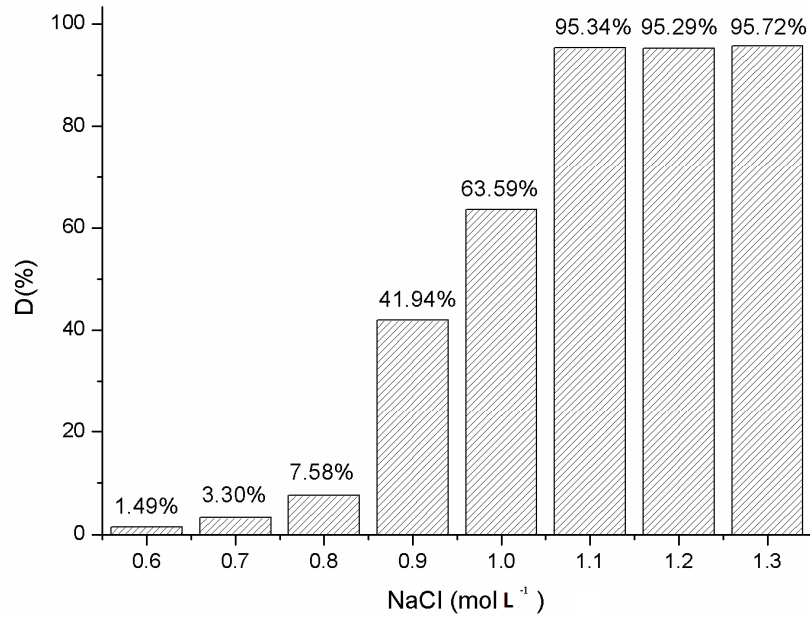
687

688

689

690

691



692

693

**Fig. 8** Desorption BSA from the surfaces of [Simam][Cl]-MNPs experiment.

694

695

